

## The continental slope current system between Cape Verde and the Canary Islands

JESÚS PEÑA-IZQUIERDO<sup>1</sup>, JOSEP L. PELEGRÍ<sup>1</sup>, MARIA V. PASTOR<sup>1</sup>,  
PAOLA CASTELLANOS<sup>1</sup>, MIKHAIL EMELIANOV<sup>1</sup>, MARC GASSER<sup>1</sup>,  
JOAQUÍN SALVADOR<sup>1</sup> and EVARIST VÁZQUEZ-DOMÍNGUEZ<sup>1,2</sup>

<sup>1</sup> Departament d'Oceanografia Física, Institut de Ciències del Mar, CSIC, Passeig Marítim de la Barceloneta 37-49,  
08003 Barcelona, Spain. E-mail: susope@icm.csic.es

<sup>2</sup> Present address: Instituto Español de Oceanografía, Centro Oceanográfico de Gijón, Camín de L' Arbeyal s/n,  
33212 Xixón, Asturias, Spain.

**SUMMARY:** We use hydrographic, velocity and drifter data from a cruise carried out in November 2008 to describe the continental slope current system in the upper thermocline (down to 600 m) between Cape Verde and the Canary Islands. The major feature in the region is the Cape Verde Frontal Zone (CVFZ), separating waters from tropical (southern) and subtropical (northern) origin. The CVFZ is found to intersect the slope north of Cape Blanc, between 22°N and 23°N, but we find that southern waters are predominant over the slope as far north as 24°N. South of Cape Blanc (21.25°N) the Poleward Undercurrent (PUC) is a prominent northward jet (50 km wide), reaching down to 300 m and indistinguishable from the surface Mauritanian Current. North of Cape Blanc the upwelling front is found far offshore, opening a near-slope northward path to the PUC. Nevertheless, the northward PUC transport decreases from 2.8 Sv at 18°N to 1.7 Sv at 24°N, with about 1 Sv recirculating offshore just south of Cape Blanc, in agreement with the trajectory of subsurface drifters. South of the CVFZ there is an abrupt thermohaline transition at  $\sigma_\theta=26.85 \text{ kg m}^{-3}$ , which indicates the lower limit of the relatively pure (low salt and high oxygen content) South Atlantic Central Water (SACW) variety that coexists with the dominant locally-diluted (salinity increases through mixing with North Atlantic Central Water but oxygen diminishes because of enhanced remineralization) Cape Verde (SACWcv) variety. At 16°N about 70% of the PUC transport corresponds to the SACW variety but this is transformed into 40% SACWcv at 24°N. However, between Cape Verde and Cape Blanc and in the  $26.85 < \sigma_\theta < 27.1$  layer, we measure up to 0.8 Sv of SACWcv being transported south. The results strongly endorse the idea that the slope current system plays a major role in tropical-subtropical water-mass exchange.

**Keywords:** boundary circulation, continental slope, northwest Africa, Poleward Undercurrent, central water mass, Cape Verde frontal system.

**RESUMEN:** EL SISTEMA DE CORRIENTES DE TALUD CONTINENTAL ENTRE CABO VERDE Y LAS ISLAS CANARIAS. – En este trabajo describimos el sistema de corrientes en la termoclina superior (hasta los 600 m) a lo largo del talud continental entre Cabo Verde y las Islas Canarias utilizando datos hidrográficos, de velocidad y de boyas de deriva obtenidos durante una campaña realizada en noviembre de 2008. La principal característica de la región es el Frente de Cabo Verde (Cape Verde Frontal Zone, CVFZ), que separa aguas de origen tropical (meridional) y subtropical (septentrional). A lo largo del talud el CVFZ suele situarse al norte de Cabo Blanco, entre 22 y 23°N, pero durante la campaña observamos sobre el talud y hasta 24°N una predominancia de aguas de origen meridional. Al sur de Cabo Blanco (21.25°N) la Corriente Subsuperficial hacia el Polo (Poleward Undercurrent, PUC) se observa como un flujo bien pronunciado (de 50 km de anchura), alcanzando los 300 m de profundidad e indistinguible de la superficial Corriente de Mauritania (Mauritanian Current, MC). Al norte de Cabo Blanco, el frente de afloramiento se encuentra alejado mar adentro, lo que facilita a la PUC seguir hacia el norte a lo largo del talud. Aún así, este transporte hacia el norte de la PUC se reduce de 2.8 Sv en 18°N hasta 1.7 Sv en 24°N, con alrededor de 1 Sv recirculando mar adentro justo al sur de Cabo Blanco, en coincidencia con las trayectorias de los derivadores subsuperficiales. Al sur del CVFZ se observa una marcada transición termohalina en  $\sigma_\theta=26.85$ . Esta transición indica el límite inferior de la relativamente pura (poco salada y rica en oxígeno) variedad de masa de agua Central Suratlántica (South Atlantic Central Water, SACW), la cual coexiste con la localmente dominante y diluida (más salada debido a la mezcla con NACW pero pobre en oxígeno por una intensificación de la remineralización) variedad de Cabo Verde (SACWcv). A 16°N

alrededor del 70% del agua transportada por la PUC corresponde a SACW mientras que a 24°N se ha transformado en un 40% de SACW<sub>v</sub>. En cambio, entre Cabo Verde y Cabo Blanco y en la capa  $26.85 < \sigma_\theta < 27.1$ , medimos un transporte de SACW<sub>v</sub> hacia el sur de hasta 0.8 Sv. Estos resultados apoyan firmemente la idea de que el sistema de corrientes de talud desempeña un papel esencial en el intercambio de masas de agua entre los regímenes tropical y subtropical.

*Palabras clave:* circulación de frontera, talud continental, África Noroccidental, Corriente Subs superficial hacia el Polo, masa de agua central, Sistema Frontal de Cabo Verde.

## INTRODUCTION

The physical oceanographic importance of continental slopes lies mainly in the fact that many major ocean currents, known as boundary currents, flow over them. The continental slopes underlie a relatively minor fraction of the world's oceans but they are the actual boundaries of the permanent upper-thermocline waters. The east and west slopes of all continents break the dominant zonal circulation in this upper ocean, forcing the flow to recirculate meridionally, often along isobaths as narrow jets.

The upper thermocline along the continental slope off NW Africa is particularly complex as it runs from subtropical to tropical regions. It spans the top 600 m of the water column, occupied by waters formed in central regions of subtropical gyres, or central waters. The major water contrast takes place at the Cape Verde Frontal Zone (CVFZ), which stretches approximately from the Cape Verde Islands to Cape Blanc (Kawase and Sarmiento 1984, Zenk *et al.* 1991, Pastor *et al.* 2008). North of the CVFZ there is a dominance of North Atlantic Central Water (NACW), of northern subtropical origin; south of the CVFZ the waters have a much more distant origin, originally coming from the subtropical South Atlantic but becoming largely modified after a long journey in the tropical regions (Fig. 1a). Pastor *et al.* (2012) emphasized that the top 300 m south of the CVFZ have characteristics close to equatorial waters, therefore being even more distinct from NACW.

The NACW flows southwards as the Canary Current (CC) until it reaches the CVFZ, where it departs offshore as the North Equatorial Current (NEC). South of the CVFZ the upper thermocline is meteorologically driven by seasonal changes in the Intertropical Convergence Zone (ITCZ). The cyclonic winds cause positive Ekman pumping, which drives offshore upwelling, the outcome being the Guinea Dome (GD) and the associated cyclonic circulation (Richardson and Walsh 1986, Peterson and Stramma 1991, Siedler *et al.* 1992). In idealized classical thermocline theories the region south of the CVFZ has been named the shadow zone (Luyten *et al.* 1983, Kawase and Sarmiento 1985), as subducting waters in the subtropical gyre cannot reach this region; the CVFZ has therefore been thought to be an effective barrier to the large-scale flow, between NACW and southern waters, although several studies have shown the presence of substantial interleaving and intermittent eddy mixing (e.g. Barton 1987, Zenk *et al.* 1991).

In summer the ITCZ moves north and the wind regime follows it. Two transatlantic eastward zonal jets, the North Equatorial Undercurrent (NEUC) at about 4°N and the North Equatorial Counter Current (NECC) approximately along 8°N, intensify and feed the southern portion of a relatively large summer GD (Siedler *et al.* 1992, Lazaro *et al.* 2005, Stramma *et al.* 2005). In winter the ITCZ moves south and the NECC weakens (Stramma and Schott 1999, Larnkhorst *et al.* 2009). South of the CVFZ, the cyclonic winds remain intense but move southeast, their centre being located near-shore (Nykjaer and Van Camp 1994). Since the GD is forced by the wind field it follows the seasonal ITCZ displacements, hence moving southeast from summer to winter (Nykjaer and Van Camp 1994). As a result, the northward along-slope flow between Cape Verde and Cape Blanc, sometimes named the Mauritania Current (MC) (Mittelstaedt 1976, Lazaro *et al.* 2005), intensifies in summer and weakens in winter (Mittelstaedt 1991).

Over the continental African slope there is yet another frontal system: the wind-induced coastal upwelling system. This is a relatively shallow system that occupies the depth of direct wind influence, typically no more than 200 or 250 m. The region between Cape Blanc and the Canary Islands, dominated by NACW, is characterized by year-long intense upwelling (Van Camp and Nykjaer 1991) and the associated near-slope southward Canary Upwelling Current (CUC) (Pelegrí *et al.* 2005, 2006, Mason *et al.* 2011). South of the CVFZ, upwelling is present only in winter, when the ITCZ migrates south. The essential elements of the upwelling system are (i) westward (offshore) Ekman transport of the surface mixed-layer waters; (ii) subsurface compensating eastward (onshore) flow which upwells over the slope due to the coastal constraint; (iii) southward (along-slope) baroclinic flow linked to the frontal system; and (iv) a large-scale pressure gradient created by the southward winds, which induces an along-slope subsurface current, known as the Poleward Undercurrent (PUC) (Barton 1989). In winter the southward winds intensify the PUC south of Cape Verde, effectively becoming the winter counterpart of the near-surface MC.

Along-slope poleward undercurrents are ubiquitous features in all major eastern boundary current systems. The northeastern Atlantic PUC was studied mostly during the 1970s and 1980s when an intense international research effort was made to understand the NW Africa upwelling system (for a review see

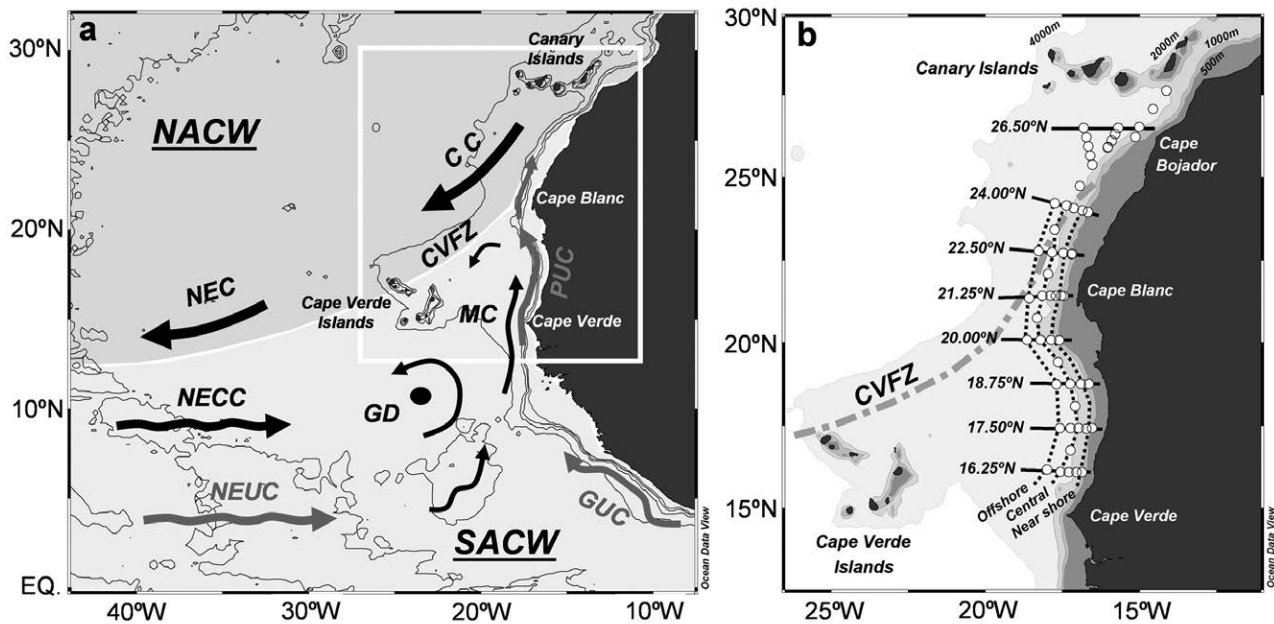


FIG. 1. – Left panel: Schematic pattern of the circulation showing the main currents and dynamic features: Canary Current (CC), North Equatorial Current (NEC), North Equatorial Counter Current (NECC), North Equatorial Under Current (NEUC), Poleward Undercurrent (PUC), Mauritania Current (MC), Guinea Undercurrent (GUC), Guinea Dome (GD) and Cape Verde Frontal Zone (CVFZ). Right panel: Map of the study area showing the hydrographic stations and the cross and along-slope sections used in this work. Contours of 500, 1000, 2000 and 4000 m isobaths are grey coloured. The near-shore and central meridional sections approximately follow the 1000 and 2000 m isobaths

Machín *et al.* 2006). The PUC is normally observed as a narrow jet (about 50 km wide) leaning on the continental slope and centred between 100 and 300 m; the poleward flow is sometimes observed to extend much deeper, to intermediate waters (Barton 1989, Machín *et al.* 2006, Machín and Pelegrí 2009). The PUC appears as a natural extension of the westward Guinea Undercurrent (GUC) and the summer MC, but it also incorporates water recirculating around the GD. The PUC has been traditionally linked to the advection of pure South Atlantic Central Water (SACW), even beyond Cape Blanc, where it encounters the CC (Mittelstaedt 1976, 1983, Tomczak and Hughes 1980, Hagen 2001).

In this study we aim to provide a detailed description of the complex system of currents over the continental slope on the eastern margin of the North Atlantic Ocean, from Cape Verde to the Canary Islands (about 16°N to 27°N). We will do so through a set of measurements taken in November 2008, with eight high-resolution cross-slope transects and several along-slope sections. First, we present the collected data set and the sea-surface wind fields during the cruise. This is followed by a brief review of a recent water-mass composition analysis carried out by Pastor *et al.* (2012), to be used in this paper. The subsequent sections are the heart of this paper, in which we explore the velocity field and the distribution of water properties over the continental slope. The purpose is to draw a picture of the circulation patterns over the continental slope and their role in the propagation of water masses of southern and northern origin.

## DATA SET

The CANOA08 cruise was carried out in November 2008 onboard the R/V *Sarmiento de Gamboa*. A total of 55 stations were occupied along the NW Africa coast from Cape Verde to the Canary Islands (Fig. 1b). Except for the first nine northeastern-most stations, which were done between 9 and 12 November, all stations were carried out between 20 and 29 November, with the vessel travelling from south to north. A total of eight cross-slope sections were completed, typically with five stations each, separated by about 1.25° of latitude; an additional station was taken between sections approximately over the 2000 m isobath. The resolution in the cross-slope direction increased from 30 km offshore to 5 km near-shore while the resolution in the along-slope direction was about 60 km over the 2000 m isobath; two additional along-slope sections, with half this resolution, may be constructed offshore and over the 1000 m isobath as far north as 24°N, as shown in Figure 1. Additionally to the hydrographic measurements, several subsurface buoys (dragged at 100 m depth) were deployed.

The stations were sampled using SeaBird 911 Plus conductivity-temperature-depth (CTD) sensors and an SBE-43 dissolved oxygen (O<sub>2</sub>) sensor. The CTD-O<sub>2</sub> probe was mounted on a 24 Niskin bottles rosette that collected water samples at standard depths. These samples were analysed for dissolved oxygen onboard and samples were frozen for a posterior analysis of inorganic nutrients. Oxygen from the bottle samples was determined by the Winkler titration method. The rela-

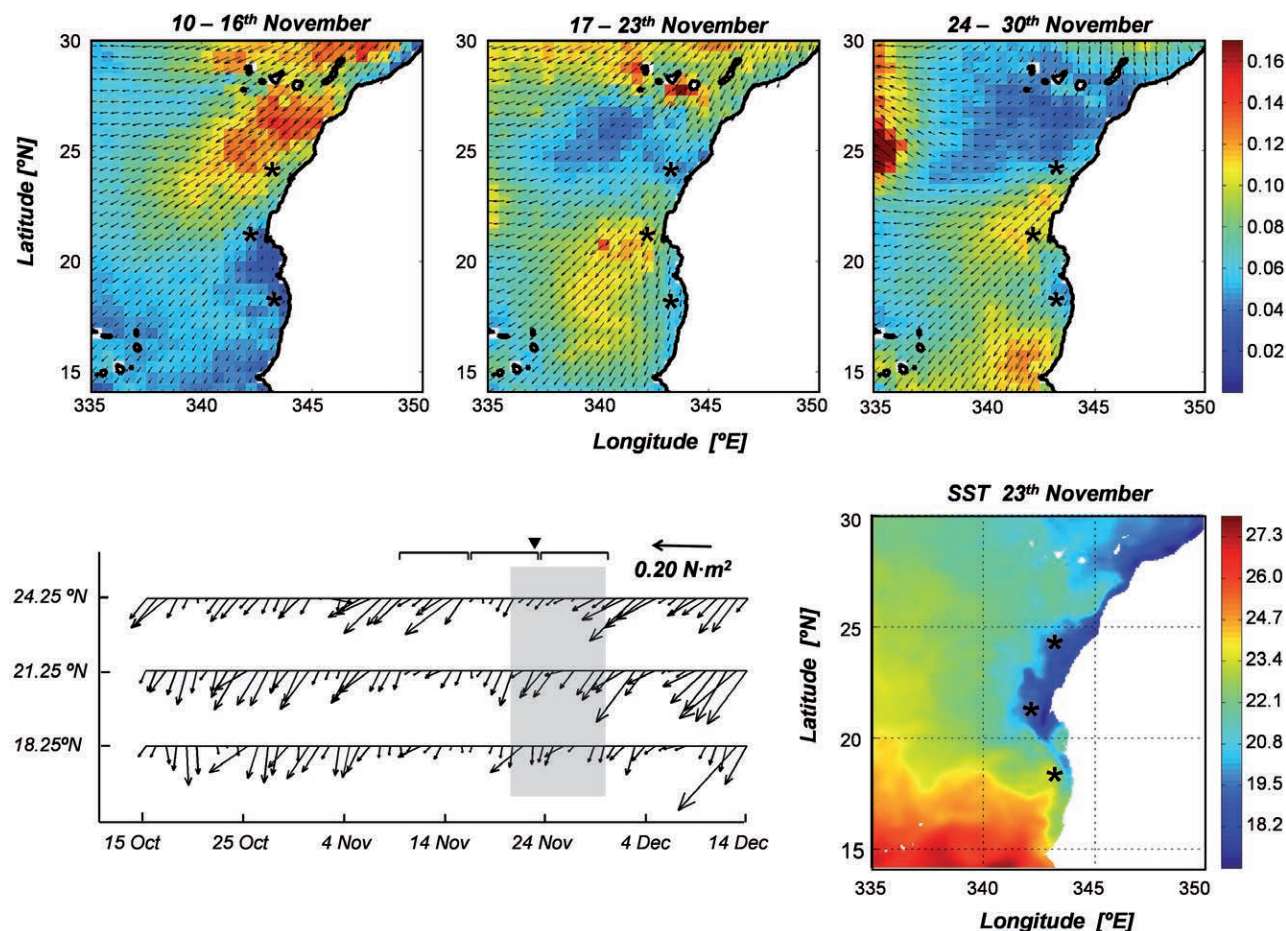


Fig. 2. – Top panels: Weekly-averaged wind stress fields [ $\text{N m}^{-2}$ ] for three consecutive weeks, starting on 10, 17 and 24 November 2008. Bottom left panel: Temporal series of the surface wind stress vector at three different latitudes over the slope (asterisks in top panels). The shaded area, the top brackets and the tick mark indicate the duration of the cruise, the average intervals for the wind stress field, and the day of the SST image, respectively (source: QuikSCAT). Bottom right panel SST [ $^{\circ}\text{C}$ ] on 23 November 2008, as obtained from OSTIA.

tion between the oxygen determined by the electrode in the CTD and the Winkler method was significant ( $r^2 > 0.96$ ,  $P < 0.01$ ,  $n > 12$ ), and the average difference between the oxygen from the CTD and the Winkler method was  $-0.63 \text{ ml l}^{-1}$ .

The velocity of the upper ocean currents was measured with a 75-kHz shipboard Ocean Surveyor Acoustic Doppler Current Profiler (OS-ADCP), which sampled the top 600 m of the water column with a good signal-to-noise ratio. The OS-ADCP was configured to produce five-minute average velocity profiles and collected single-ping data with a vertical resolution of 8 m at 75 kHz. The ADCP was initially calibrated over the continental shelf through bottom tracking so that the alignment angle and scale factor were determined; later, from the comparison of consecutive repeated sections in a region of high horizontal shear, a meridional velocity offset of  $0.02 \text{ m s}^{-1}$  was detected and the velocity field was corrected. A Lowered ADCP (LADCP) system, consisting of two RDI 300 kHz Workhorse Monitors used in synchronized master-slave mode, was also mounted on the rosette but it did not work properly at all stations. Nevertheless, a comparison between the

available LADCP profiles and the corrected on-station ADCP data shows good agreement (not shown) and gives us confidence in the good quality of this ADCP data set. Therefore, in this study a velocity profile is calculated at each station by averaging all ADCP data collected while the vessel was on that position.

The surface wind field, prior to and during the execution of the experiment, was extracted from the QuikSCAT data set (Fig. 2). We may appreciate a predominance of north-easterly winds during the cruise over the whole study area. During the first week of measurements the wind was quite intense north of Cape Blanc; during the second and third weeks it weakened and intensified north and south of Cape Blanc, respectively. For the time period of the cruise, the sea surface temperature (SST) field was available in near-real time through the Operational SST and Sea Ice Analysis (OSTIA) product (Stark *et al.* 2007).

#### OPTIMUM MULTI-PARAMETRIC ANALYSIS

An Optimum Multi-Parameter (OMP) method aims to find the contribution of different predefined source

water types in a water sample. These contributions are determined as a linear mixing combination in a multi-parameter space (Mackas *et al.* 1987, Tomczak and Large 1989). Each parameter is given a different weight according to its accuracy and natural variability. In this study we follow the application of the OMP for the NW Africa region, as presented in Pastor *et al.* (2012). Five independent variables (potential temperature, salinity, oxygen, phosphate and silicate) are combined with mass conservation, and a total of six water types are specified. The analysis is applied to data in the density range  $26.46 < \sigma_\theta < 27.82$ , specifically excluding near-surface data (down to about 100 or 150 m) in order to avoid atmospheric and biogeochemical processes (hereafter we use sigma-theta or potential density anomaly, equal to potential density less 1000, in units of  $\text{kg m}^{-3}$ ).

One relevant contribution of Pastor *et al.* (2012) was the distinction of two different varieties of southern waters, predominantly found in the region south of CVFZ. While the regional central water mass of southern origin was defined by Tomczak (1981), a fresher and colder variety, therefore with purer South Atlantic characteristics, may also be detected from historical observations in the southeastern North Atlantic (Voituriez and Chuchla 1978). The distinction between the two varieties allows us to discern the different contribution of both water masses to the slope undercurrent. Therefore, hereafter we refer to the regional variety as Cape Verde South Atlantic Central Water (SACWcv), defined in the OMP analysis by the contribution of two water types (upper and lower Cape Verde South Atlantic Central Water, SACWcv-u and SACWcv-l respectively); in contrast, the purer variety is simply named South Atlantic Central Water (SACW), being solely represented by one point in the multi-parameter space (one water type) due to its shallowness, as we discuss in the next sections. The contribution of NACW is assessed again through the combination of two points,

the upper and lower NACW (NACW<sub>u</sub>, NACW<sub>l</sub>). Figure 3a shows the location of these northern and southern central waters in a temperature-salinity diagram. Additionally, the presence of Antarctic Intermediate Water (AAIW) was also introduced in the analysis to properly describe the water masses distribution at the bottom of the thermocline; however we will not use it in this paper.

## PENETRATION OF SACW CHARACTERISTICS

In this section we examine the latitudinal dependence of mean water properties with the help of scatter plots, where the spatial variability is smoothed out through a reduced data interpolating variational analysis (DIVA) technique (Figs. 3b, c). These plots do not aim to examine the detailed distribution of water properties but rather to view the gross latitudinal property patterns.

The most outstanding feature of the hydrographic field is the clear distinction between northern and southern central waters (Fig. 3a). At the southernmost part of the region, for  $\sigma_\theta < 26.85$  we may distinguish the presence of the fresher and more oxygenated SACW; the further south the more oxygen we find at these upper levels. In contrast, at the northern end we find only NACW; on the same isopycnal surface, NACW is a much saltier, colder and oxygen-richer water mass than the southern water masses. However, the most common water in the shadow zone is the regional SACWcv variety, which is substantially saltier than SACW. Furthermore, the SACWcv has the lowest oxygen concentrations of the three central water masses (Fig. 3b), suggesting that the SACWcv water mass is an old SACW variety that has lost most of its oxygen content while also mixing slowly with the nearby salty NACW. The SACW variety thus represents a relatively young water mass that renovates the upper layers of the shadow zone through direct advec-

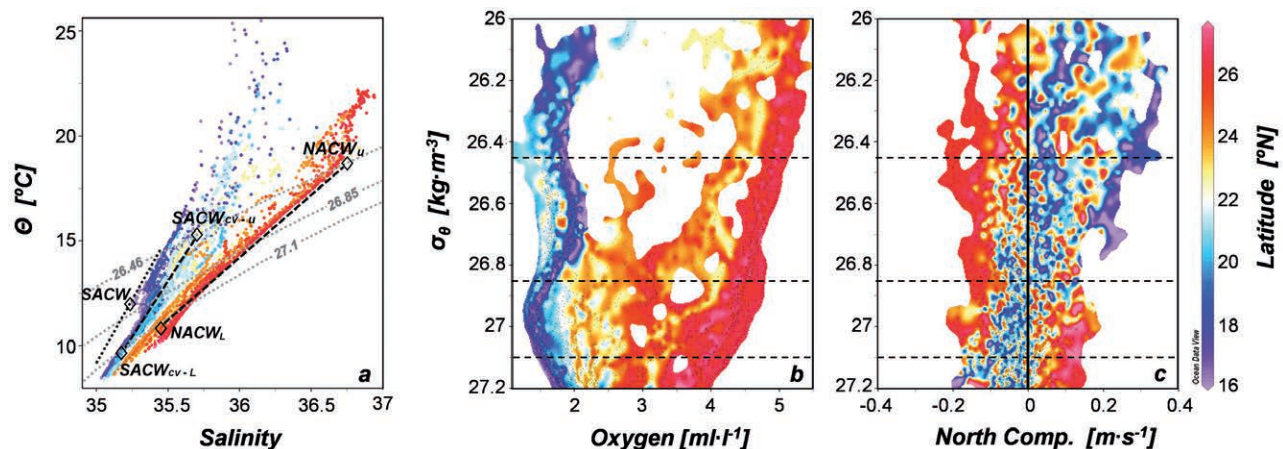


FIG. 3. – Left panel. Potential temperature-salinity diagram as obtained using the whole data set. Void diamonds indicates the water types used in the OMP analysis of Pastor *et al.* (2011). Central and right panels: Smoothed scatter plots, again obtained using the whole data set, of dissolved oxygen and meridional velocity (in  $\text{m s}^{-1}$ , positive northwards) as a function of potential density. In all plots the latitude [ $^{\circ}\text{N}$ ] is colour-coded according to the right-hand-side colour bar.

tion of the tropical eastward zonal jets, the NEUC and NECC (Elmoussaoui *et al.* 2005).

Another prominent characteristic is the vertical salinity minimum observed at  $\sigma_\theta=26.8$ , an abrupt salinity, and even temperature, inversion at depth. This salinity minimum matches with the point of SACW definition and is also found just a little deeper than the subsurface oxygen maximum (Fig. 3). These features may be detected in salinity distributions presented by several authors for the region south of the CVFZ (e.g. Tomczak 1972, Fraga 1974, Hughes and Barton 1974) but few studies have yet explored its significance. Voituriez and Chuchla (1978) early proposed that this salinity minimum represents a boundary between northward flow of SACW in upper layers and southward flow of NACW deeper. More recently, Elmoussaoui *et al.* (2005) used a high-resolution model to highlight the existence of a thermohaline transition (smoothed in their numerical solution) at  $\sigma_\theta=26.8$ . The numerical outputs suggests that the NEUC and NECC merge southwest of the GD, from where they reach towards the African slope and recirculate north towards the CVFZ. However, these shallow jets may only ventilate the shadow zone down to some 300 m, i.e. the lower portion of the upper thermocline is not renewed, so its waters have long residence time, leading to high remineralization and low oxygen concentrations (Kartensen *et al.* 2005, Stramma *et al.* 2005, 2008). A scatter plot of the meridional velocity interpolated as a function of density illustrates the predominant propagating directions of southern and northern waters (Fig. 3c); the interpolation smoothes out the velocity fields so that, despite the existence of high spatial variability, we may identify mean flow patterns. The meridional velocity component has a similar depth transition, in agreement with Voituriez and Chuchla (1978). All the way until 22.5°N, the layers with  $\sigma_\theta<26.85$  move predominantly northwards at speeds of up to 0.3 m s<sup>-1</sup>, carrying oxygen with SACW characteristics. This northward flow reaches significantly north of Cape Blanc, i.e. past the traditional interjection of the CVFZ with the continental slope. At 24°N the flow is approximately null and further north it appears to reverse but is obscured because of the mesoscalar variability south of the Canary Islands. Contrarily, at latitudes south of Cape Blanc the deeper layers ( $26.85\leq\sigma_\theta<27.1$ ) move predominantly southwards, carrying SACWcv characteristics. North of Cape Blanc, these deep layers do not display a predominant propagation pattern. Hence, near the CVFZ there is substantial convergence in layers shallower than  $\sigma_\theta=26.85$  and weak divergence below.

According to the above observations, following Elmoussaoui *et al.* (2005), we can distinguish between surface waters (SW;  $\sigma_\theta<26.46$ , down to about 100 m), upper central waters (uCW;  $26.46\leq\sigma_\theta<26.85$ , between about 100 and 300 m) and lower central waters (lCW;  $26.85\leq\sigma_\theta<27.1$ , between about 300 and 500 m). We set the interface between uCW and lCW slightly deeper than in Elmoussaoui *et al.* (2005), i.e.

$\sigma_\theta=26.85$  rather than 26.8, in order to better match the observed abrupt vertical transition in southern water characteristics and to include the full low-salinity SACW signal within the uCW.

## CROSS-SLOPE SECTIONS

Despite the general smoothed picture arising from Figure 3c, the slope current system shows high spatial variability. In order to appreciate this variability and to identify the propagating paths, we examined the distributions of salinity, oxygen, meridional velocity and water-mass composition in eight cross-slope sections at nominal latitudes of 16.25, 17.5, 18.75, 20.0, 21.25, 22.5, 24.0 and 26.5°N (Figs. 4 and 5).

Trade winds were present during the whole cruise, leading to intense upwelling off NW Africa, as illustrated by the SST image in Figure 2. South of Cape Blanc upwelling is the result of the predominant local winds, but the uCW and SW layers still display a considerable northward along-slope flow which may be interpreted as a late expression of the summer MC on top of the PUC. North of Cape Blanc, upwelling is very intense and located far offshore, probably arising from the build-up of wind impulses during the summer-long upwelling season (e.g. Csanady 1977). The combination of these two features should allow the propagation of the PUC, manifested as a northward flow within SW and uCW layers, well beyond Cape Blanc. Figure 4 indeed shows a well-defined northward flow attached to the continental slope, with maximum values in all sections above 0.2 m s<sup>-1</sup>, extending from the surface down to 300 m in the southern sections and shoaling towards the north. In this figure it is difficult to distinguish the near-surface MC from the subsurface PUC; therefore, our measurements reflect the late summer and autumn conditions south of Cape Blanc, when the MC is strengthened (Mittelstaedt 1976) and northward transport is maximum (Elmoussaoui *et al.* 2005).

The SW layer is highly influenced by the upwelling system. Within this layer the contours of all properties uplift towards the slope, except for the relatively low oxygen content as a sign of high productivity (Fig. 5). A marked change in properties is observed just north of Cape Blanc (Fig. 5f), denoting the location of the CVFZ. The surface flow has a predominant northward direction in all cross-slope sections (Fig. 4), typically wider than 50 km; in the southern sections this could be interpreted as the MC, while beyond Cape Blanc it must be the surface manifestation of the PUC. North of Cape Blanc, the offshore extreme of these 100-km-wide sections flows south (Fig. 4), probably related to the far offshore location of the coastal upwelling jet during the intense upwelling season (Fig. 3). At 26.5°N, south of the Canary Islands, the flow is dominated by intense mesoscalar activity. The near-slope high salinity and oxygen values at 22.5°N, north of Cape Blanc, suggest that the flow direction at the CVFZ is intermittent, be-

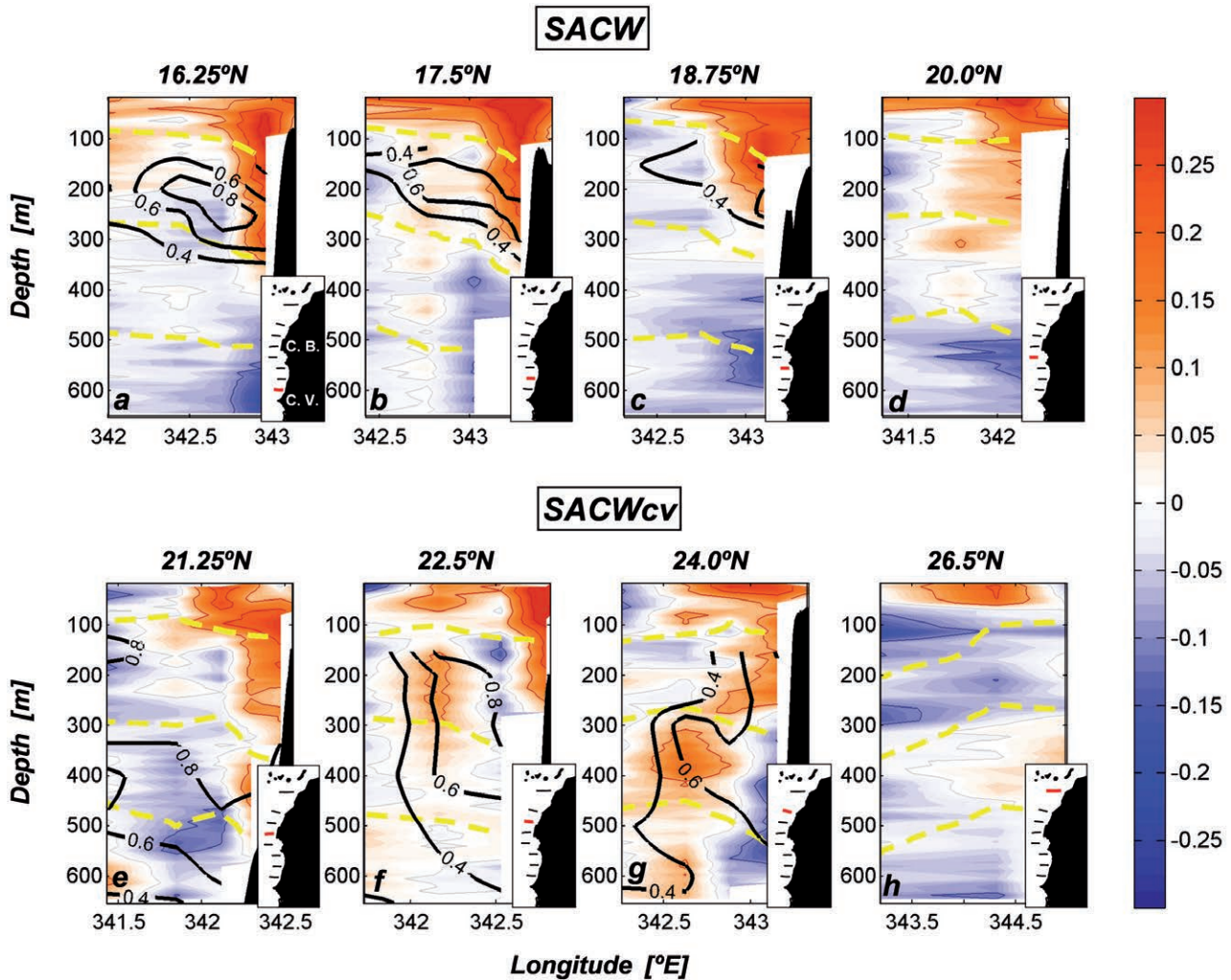


FIG. 4. – Distribution of water masses on eight different cross-shore sections (Fig. 1). The meridional velocity (in  $\text{m s}^{-1}$ ) is colour-coded according to the right-hand-side colour bar, with positive values denoting northward flow; contours are drawn every  $0.1 \text{ m s}^{-1}$  interval. The black lines show either the fraction of SACW south of Cape Blanc (top panels) or the fraction of SACWcv north of Cape Blanc (bottom panels); in the upper panels the remaining water-mass contribution is only SACWcv, while in the lower panels it is NACW. Three selected isopycnals (26.46, 26.85 and 27.1) are drawn in yellow. The map insets indicate the location of the corresponding section.

ing northward during the cruise but having possibly changed direction at previous times. It is therefore possible that the  $22.5^\circ\text{N}$  latitude corresponds to a mean northern limit of the MC, in agreement with the results of Lazaro *et al.* (2005).

The uCW layer is characterized by the presence of the PUC in all sections except  $26.5^\circ\text{N}$  (Fig. 4). In this layer and south of the CVFZ, the slope current appears as a northward jet with a width of several tens of kilometres, which reaches down to over 200 m and is hardly distinguishable from a slightly wider surface MC. South of about  $20^\circ\text{N}$  the uCW layer appears as an oxygen maximum stratum, with values as high as  $2.12 \text{ ml l}^{-1}$  (Fig. 5). This high oxygen content is related to the predominance of SACW, which is present only in this layer. The presence of SACW is progressively reduced as we move north along the slope, with decreasing oxygen content. Mixing with salty NACW is responsible for the significant salinity increase near Cape Blanc

but, though NACW is higher in oxygen than SACWcv, the near-slope oxygen content is notably reduced. Near the Cape Blanc filament the near-slope subsurface oxygen level is further exhausted, with values as low as  $1.14 \text{ ml l}^{-1}$  (Fig. 5e), and the offshore waters appear slightly more oxygenated. This suggests that the CVFZ prevents some of the southern waters from flowing north of Cape Blanc, this becoming an area where SACWcv is formed through mixing of SACW with NACW and enhanced oxygen consumption of SACW (because of remineralization taking place under the highly productive upwelled waters). Despite the blockage of the CVFZ, some of this oxygen-poor and relatively salty SACWcv is transported along the slope by the PUC (Figs. 4f and 5f) and released as far north as Cape Bojador (Fig. 4g).

The northeastward extension of the NEUC slowly advects SACW to the northern part of the GD in summer, but only a fraction of this relatively pure SACW

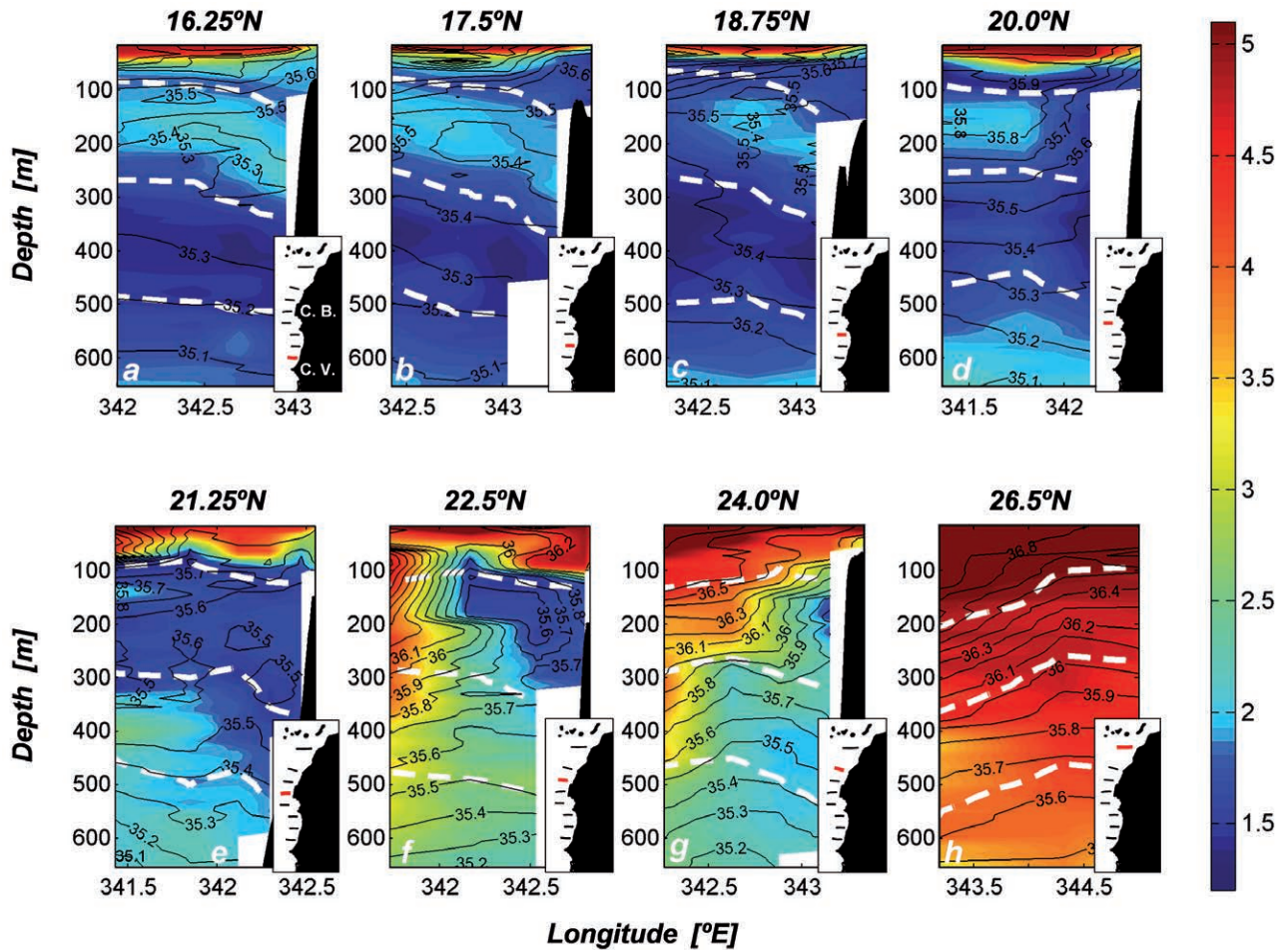


Fig. 5. – Distributions of oxygen content ( $\text{ml l}^{-1}$ , coloured) and salinity (black contours) on eight cross-shore sections. Three selected isopycnals (26.46, 26.85 and 27.1) are shown as dashed white lines. The map insets indicate the location of the corresponding section.

is eventually incorporated by the relatively shallow PUC (which occupies the uCW). The core of SACW is located seawards from the PUC core, in agreement with observations by Tomczak and Hughes (1980), in some cross-slope sections coinciding with the presence of a weak southward flow (Figs. 4a, b). Therefore, it appears that most of the SACW inflow may recirculate between the continent and the Cape Verde Islands and that the PUC is not always directly fed by SACW, hence validating the numerical results of Elmoussaoui *et al.* (2005). In most sections the dominant water mass advected by the PUC is the recirculating SACWcv (Figs. 4 and 5), although it has a large SACW contribution that arises from the extension of the tropical zonal jets, and possibly also from the low-latitude along-slope Guinea Undercurrent (Mittelstaedt 1976). North of Cape Blanc the southern central waters, already fully transformed into SACWcv, penetrate northwards through the along-slope PUC (Fraga 1974, Tomczak 1981, Hagen 2001). The salinity distributions for the cross-shore sections between 21.25°N and 24.0°N show that this intrusion occupies a 50- to 100-km-wide near-slope meridional band. Such a PUC penetration

is likely favoured by the high intensity of upwelling during the previous weeks or months (Fig. 3), so the distant offshore position of the upwelling front is coupled to the propagation of relatively fresh and cold SACWcv (Figs. 5e, f, g).

The ICW and uCW layers display quite opposite distributions south of Cape Blanc. In the lower layer the oxygen content reaches minimum values in the southern sections ( $1.27 \text{ ml l}^{-1}$ , Fig. 5), similar to those found in the GD oxygen minimum zone (Stramma *et al.* 2005), and increases towards the north under the influence of NACW. North of Cape Blanc the minimum oxygen values are found near the slope, indicative of the presence of SACWcv (Figs. 5 and 6c, g). However, a divergent flow is observed along the continental slope, with moderate (maximum  $0.15 \text{ m s}^{-1}$ ) southward flow at latitudes of less than 22°N and the presence of substantial variability further north. The existence of southward flow is counter-intuitive with the presence of waters of southern origin (SACWcv) and raises the possibility that the direction of the flow may seasonally reverse. We will come back to this issue in the next section.



## ALONG-SLOPE SECTIONS

The high cross-shore variability in the distribution of water properties is accompanied by substantial along-slope coherence (Fig. 6). This coherence is the result of the system of meridional along-slope currents although it breaks at the PUC-CC convergence region north of Cape Blanc, as well as off Cape Bojador because of intense mesoscalar activity during the cruise (Rodríguez-Marroyo *et al.* 2011). The minimum oxygen distribution depicts a vertically-tilted CVFZ which separates northern from southern central waters, with the transformation of SACW into SACWcv near the slope and interleaving of SACWcv and NACW further offshore (Fig. 6).

The velocity field along the African slope shows that SW and uCW, composed of the surface MC and a relatively shallow PUC down to 300 m depth, converge towards about 22°N. The underlying ICW layers flow towards the equator at latitudes less than 20°N and do not have a clear predominant direction at northern latitudes (Figs. 4 and 6). As stated above, the southern sections only have limited NACW influence within the ICW layers, mostly in the form of water patches (Fig. 6f), while there is a significant presence of SACWcv beyond 24°N (Fig. 6e, f, g). This finding suggests that an enhanced and deep PUC could have developed before our observations, resembling the characteristic winter flow conditions proposed by Mittelstaedt (1976).

The presence of ICW areas with NACW influence south of Cape Blanc may be related to meanders detaching from the CVFZ but its ubiquity along the slope suggests that they are caused by deep flow reversals, in instances such as those proposed by Voituriez and Chuchla (1978). The existence of an along-slope southward flow within ICW, bringing NACW south of Cape Blanc, would help explain our observations of NACW in this region, as well as the related observation of along-slope high-salinity waters in the simulations of Elmoussaoui *et al.* (2005). Such a flow, however, is not endorsed by our observations so it must be intermittent, probably seasonal.

The abrupt vertical transition between the uCW, dominated by the low-salinity SACW, and the underlying ICW, consisting almost exclusively of SACWcv, is located at about 300 m depth. This is also the depth reached by the summer-autumn PUC and by the eastward tropical jets (recall that the NECC only develops in summer-autumn), therefore suggesting that the enhanced ventilation of the uCW is related to the seasonal atmospheric forcing and the consequent regional circulation pattern. The location of the high SACW core, slightly offshore from the PUC (Figs. 4a, b), suggests that the connection between the zonal tropical jets and the PUC may not be direct, taking place instead through recirculation loops. In winter the PUC deepens and the connection with the zonal jets probably weakens; at this time the PUC would transport both regional southern water varieties.

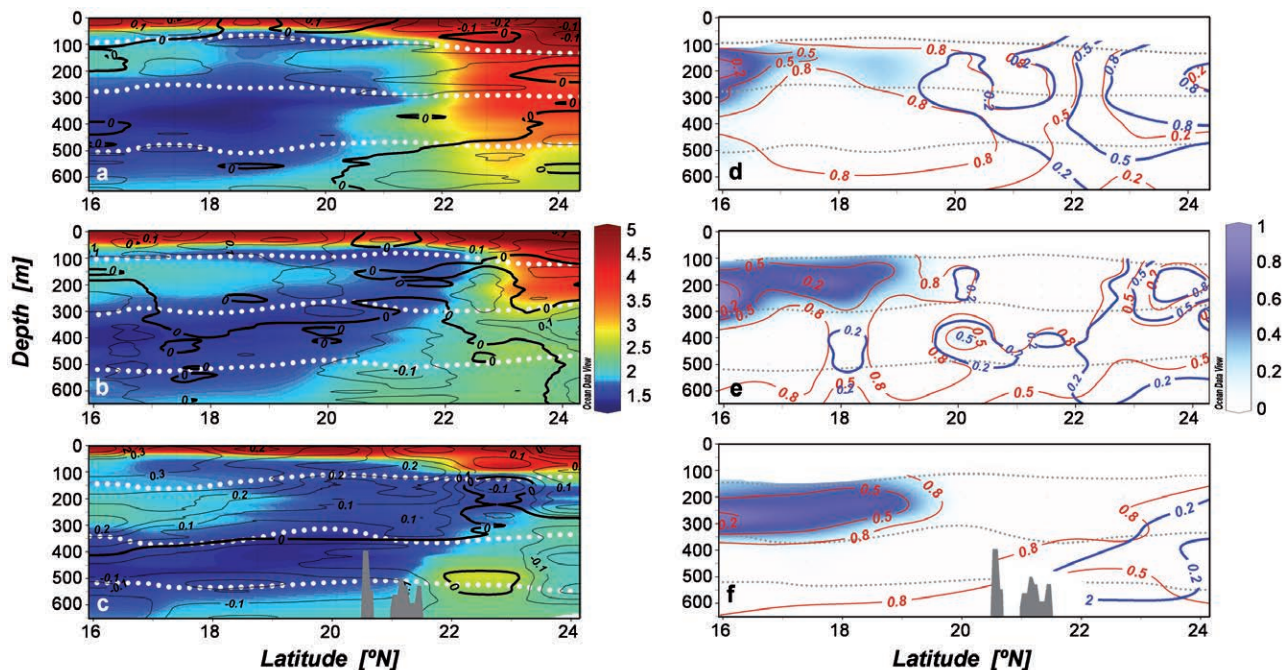


Fig. 6. – Left panels: Distributions of oxygen content ( $[\text{ml l}^{-1}]$ , colour-coded according to the right-hand-side colour bar) and meridional velocity ( $[\text{m s}^{-1}]$ , black lines, positive northward). Right panels: Contribution of three different water masses along the same sections: SACW (blue colours following the right-hand-side colour bar), SACWcv (red contours) and NACW (blue contours). Three selected isopycnals (26.46, 26.85 and 27.1) are indicated with white (grey) dotted lines in the left (right) panel. The top, central and bottom panels correspond to the along-slope sections located offshore and over the 2000 and 1000 m isobaths, respectively (Fig. 1).

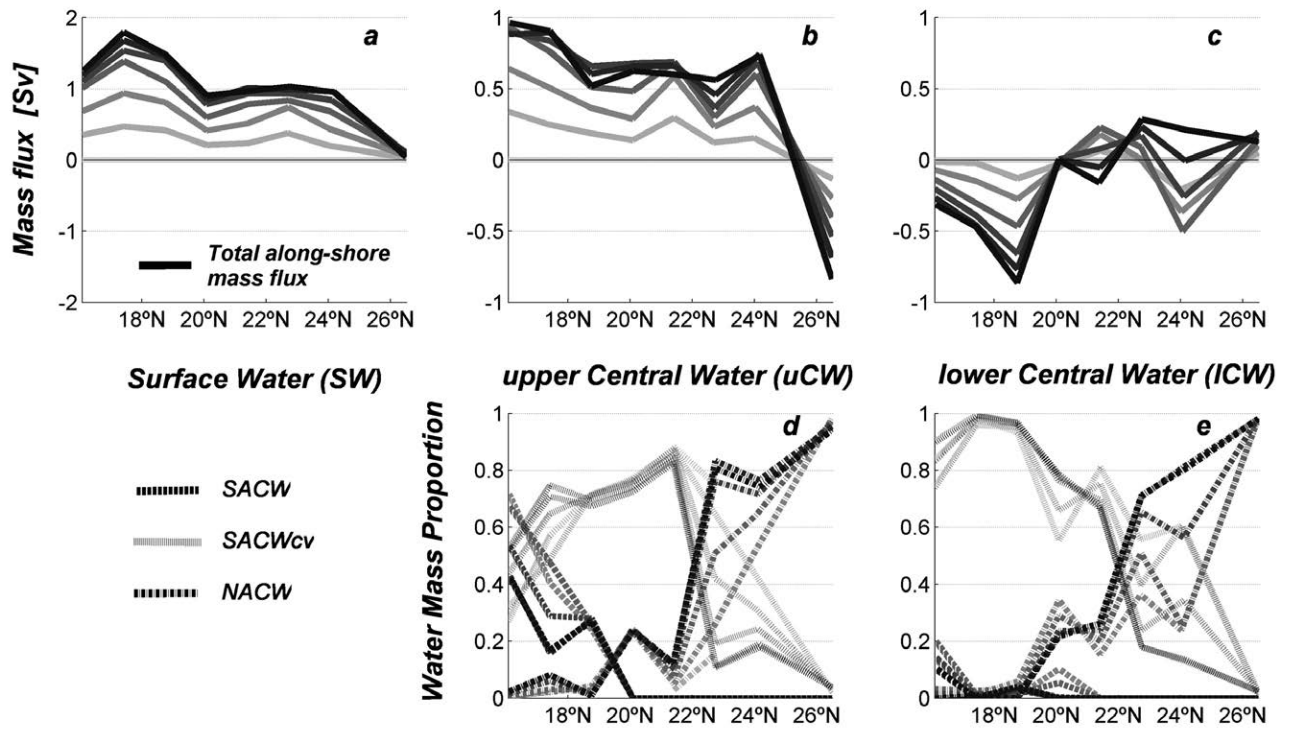


FIG. 7. – Top panels: Latitudinal change in meridional mass transport (positive northward [Sv]) for three different layers. The transports are calculated through the eight cross-shore sections, with the accumulated transports every 10 km (increasing seawards from the shelf break) represented by curves of increased darkness. Bottom panels: Average SACW, SACWcv and NACW fractions in each cross-shore section interpolated every 10 km; the increased darkness again represents the increasing seaward distance from the shelf break. Note that no OMP solution is available for SW; also note the different vertical scale for the left panel.

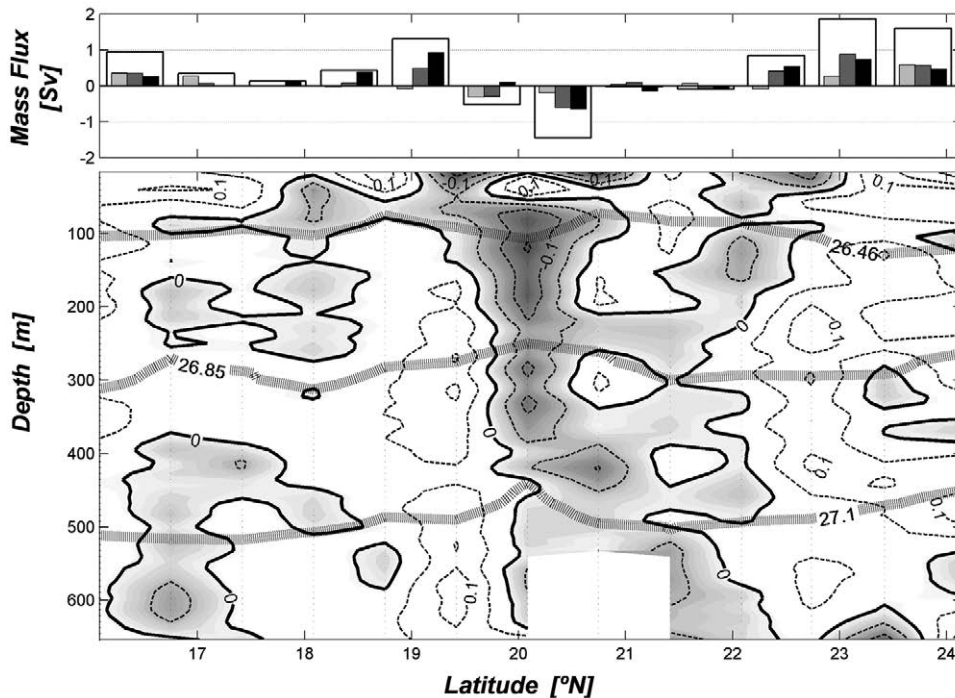


FIG. 8. – Bottom panel: Distribution of zonal velocity on the 2000-m isobath along-slope section (Fig. 1) (in  $\text{m s}^{-1}$ ; contours are drawn every  $0.05 \text{ m s}^{-1}$ ; positive values denote eastward flow, westward velocities are shaded in grey). The grey thick lines show the three selected isopycnals (26.46, 26.85 and 27.1). Top panel: Corresponding zonal transports per water stratum as calculated between each pair of stations located along the 2000-m isobath section; SW (light gray), uCW (gray), ICW (dark gray) and the total (box); positive values denote eastward transport.

The meridional mass fluxes, integrated through the cross-shore sections, are shown in Figure 7. The SW follow north through all sections, reaching up to 1.8 Sv south of the CVFZ (Fig. 7a). The uCW also move north through all sections, as a narrow jet along the continental slope, except at the northernmost section where the flow is controlled by mesoscale variability (Fig. 7b). In the southernmost section this jet transports 1 Sv with a 70% average contribution of SACW (30% of SACWcv). This transport, and the pure SACW contribution, decreases steadily northwards, turning into the SACWcv variety as it approaches the CVFZ (Fig. 7d). The maximum presence of this oxygen-poor variety is reached near Cape Blanc (80% on average). North of Cape Blanc (22°N) this southern water mass turns into the predominant NACW, although as far as 24°N there is still a northward flow of 0.7 Sv as a mixed water mass which includes 40% of SACWcv. Taking into account both the SW and the uCW layers, the maximum poleward flow reaches 2.7 Sv at 18°N and decreases to 1.7 Sv at 24°N, north of the CVFZ.

In the ICW the integrated along-slope mass transport is rather variable. South of Cape Blanc, there is a southward transport of SACWcv, its contribution reaching more than 90% and up to a maximum of 0.8 Sv (Figs. 7c, e); this water must come from the interior as near-zero along-slope transport takes place at the frontal zone. It is north of Cape Blanc (beyond 22°N) that NACW becomes the dominating water mass, particularly at the offshore stations where there is only a weak northward flow (Figs. 6a, e and 7c, e); the situation is different at the near-shore stations, where substantial SACWcv is found despite the predominance of a southward flow (Figs. 6c, g and 7c, e). This finding reinforces the idea of seasonal reversals in the deep along-slope current, as found in numerical simulations by Elmoussaoui *et al.* (2005) and reported by Machín and Pelegrí (2010) for the underlying intermediate waters.

Within an upwelling region we tend to think of the cross-shore flow as resembling an idealized vertical cell, with offshore Ekman flow in the surface layers and a compensating onshore subsurface flow. However, the above results illustrate the existence of substantial along-slope water convergence within both SW and uCW (Fig. 6), in our case this being the main factor responsible for the cross-shore circulation patterns. This is confirmed by the presence of substantial offshore flow in these two water strata, between about 19°N and 21°N (Fig. 8). The existence of water export is confirmed by the trajectories of three drifters dragged at 100 m (Fig. 9). All three drifters initially followed north along the slope and at least two of them (the third one stopped transmission) departed offshore south of the position of the CVFZ, which at the time was located as far north as 22°N to 23°N (Fig. 9). Within SW the flow pattern is more complex, probably as the result of coastal filaments and the associated recirculation patterns (Fig. 8). Finally, within the ICW layer, we find

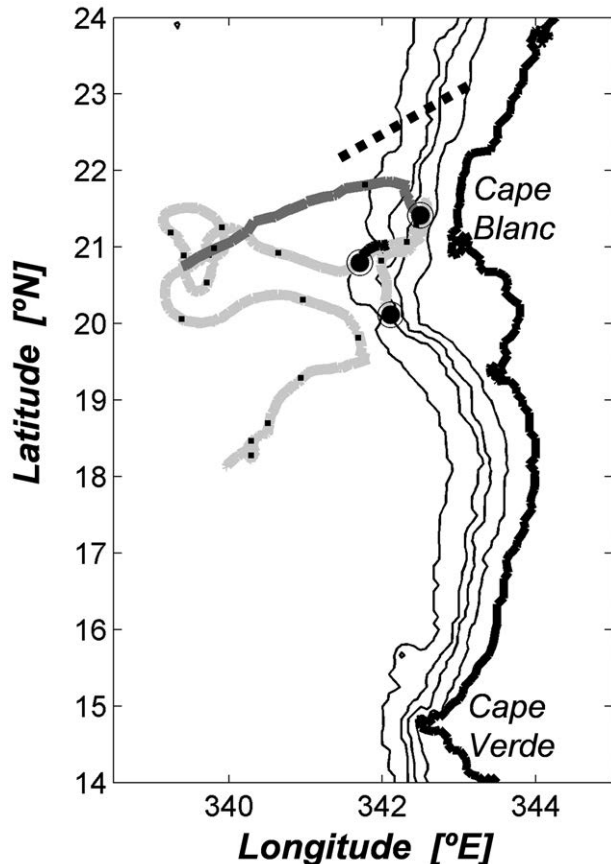


Fig. 9. – Trajectories of three buoys dragged at 100 m and deployed near Cape Blanc during the cruise. The black circles indicate the deployment positions; the black trajectory corresponds to 9 days, the dark-grey trajectory to 22 days and the light-grey trajectory to 170 days. The tick marks in the light-grey and dark-grey trajectories indicate the position every week. The thick dotted line indicates the approximate position of the CVFZ as inferred from the location of the 36.0 isohaline at 100 m (Zenk *et al.* 1991).

that waters south of 20°N recirculate onshore between 19°N and 20°N and find their way south along the slope (Figs. 7c, e). In this lower stratum there appears to be a good connection between the slope current and the interior GD ocean which gives rise to the observed southward flow of the SACWcv variety. North of 20°N another recirculation may be occurring, with onshore flow between 22.5°N and 23.5°N and offshore export between 20°N and 21°N.

#### CONCLUDING REMARKS

The comprehensive data set acquired during the CANOA08 cruise provides a good picture of what probably is the characteristic late summer and autumn circulation of surface and central waters along the continental slope between Cape Verde and the Canary Islands (Fig. 10). Two quite different dynamic regions may be distinguished, separated by the Cape Verde Frontal Zone (CVFZ), which crossed the slope at a position north of Cape Blanc (22–23°N). North of this frontal zone, the circulation

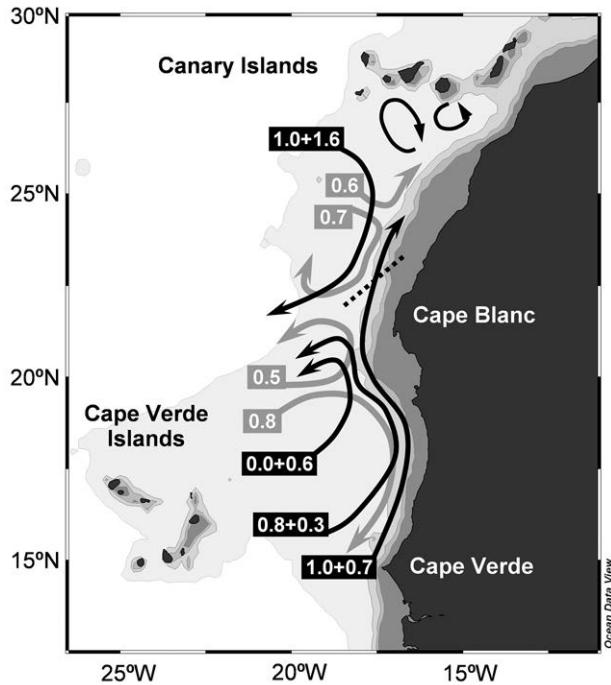


FIG. 10. – Circulation patterns and mass fluxes [Sv] of SW+uCW (black line) and ICW (grey line) during CANOA08. The thick dashed line illustrates the position of the CVFZ.

pattern is highly variable as a result of the interaction between coastal upwelling, the Poleward Undercurrent (PUC) and the intense mesoscalar activity in the region south of the Canary Islands. South of Cape Blanc the dynamics is dominated by the along-slope PUC and the surface northward branch of the cyclonic circulation around the Guinea Dome (GD), the Mauritanian Current (MC). Our dataset corresponds to a situation when maximum northward flow takes place (Mittelstaedt 1976, Elmoussaoui *et al.* 2005), thanks to an enhanced MC (up to 1.8 Sv) within surface waters (SW;  $\sigma_\theta < 26.46$ , down to about 100 m) and through a well-defined but relatively shallow along-slope PUC (1 Sv) within upper central waters (uCW;  $26.46 \leq \sigma_\theta < 26.85$ , between some 100 and 300 m). Poleward along-slope transport reaches at least  $24^\circ\text{N}$ , where we still find 1.7 Sv of SW and uCW, favoured by the far offshore position of the coastal upwelling front.

The upper-thermocline circulation in the GD region has been traditionally thought to have long residence times (Kawase and Sarmiento 1985, Zenk *et al.* 1991). Tropical water feeds the GD through the North Equatorial Undercurrent (NEUC) at about  $4^\circ\text{N}$  and seasonally also by the North Equatorial Counter Current (NECC) at about  $7^\circ\text{N}$  to  $8^\circ\text{N}$ , but this only occurs in the relatively shallow uCW layers (Elmoussaoui *et al.* 2005, Stramma *et al.* 2008). Further deep, within the lower central waters (ICW;  $26.85 \leq \sigma_\theta < 27.1$ , between about 300 and 500 m), the GD waters have much longer residence times (Kawase and Sarmiento 1985, Zenk *et al.* 1991).

How much of the NEUC and NECC connects with the PUC and how much crosses the CVFZ? The distinction of two varieties of southern central waters (relatively pure SACW and the more diluted, regional, SACWcv) has allowed us to better understand the complex processes that characterize the CVFZ. The SACW variety, characterized by a salinity minimum and relatively high oxygen content, is found only within uCW. This water type fits well the characteristics of the upper-thermocline waters at  $7.5^\circ\text{N}$  (Arhan *et al.* 1998), therefore confirming that they represent tropical waters advected eastwards by the shallow NEUC and NECC jets. These jets do not feed the continental slope currents through some specific location, as the core with the highest SACW content is found offshore from the PUC and the proportion of SACW increases progressively equatorwards, but rather the connection spreads all the way between Cape Blanc and Cape Verde and even further south. Similarly, the ICW layers appear as connected to the interior ocean through an anticyclonic gyre, possibly the eastern limb of a more closed-like system that would perpetuate the old SACWcv as the dominant water variety in the shadow zone.

Just north of Cape Verde, at  $16^\circ\text{N}$ , about 70% of the water transported by the PUC is pure SACW. On the one hand, incorporation of NACW across the CVFZ results in a salinity increase; on the other hand, high productivity in the along-slope upwelling region and the Cape Blanc giant filament (Gabric *et al.* 1993) leads to sinking of organic particles and enhanced oxygen consumption. Both processes cause the full transformation of SACW into the SACWcv variety. Some SACW is exported offshore near Cape Blanc (between about  $20^\circ\text{N}$  and  $21^\circ\text{N}$ ) and likely recirculates south; however, a large fraction of southern waters, already transformed as SACWcv, follows north along-slope, with as much as 0.7 Sv reaching at least  $24^\circ\text{N}$ . The waters located off Cape Blanc, during our cruise found just south of the CVFZ, appear to be the site of substantial mesoscale recirculations which must enhance the exchange of southern and northern waters. (Fig. 10)

Our observations at the ICW level also show that at latitudes higher than Cape Blanc there is a substantial amount of SACWcv which flows south. This raises the possibility of seasonal current reversals in this deep water stratum, in agreement with numerical simulations by Elmoussaoui *et al.* (2005). These reversals are likely to occur just after a deep PUC phase, which would previously take SACWcv north along the slope as observed on our cruise. Our results suggest that a significant fraction of the observed southward flow feeds from the interior ocean, possibly in some sort of basin-wide anticyclonic gyre, in our case not bringing much NACW south of the frontal region. However, the meridional coherence of this southward flow suggests that during similar deep reversals there could also be transfer of NACW from the subtropical to the tropical gyre. This would provide an alternative mechanism for cross-frontal exchange, which could compete with the

predominant one-way entrainment of southern waters into the subtropical gyre found by Klein and Tomczak (1994). In this study we have presented a rather novel perspective of the current system over the continental slope off NW Africa. Many previous studies have emphasized the importance of the equatorward and off-shore transport of properties by the subtropical eastern boundary system (Mittelstaedt 1983, 1991, Van Camp *et al.* 1991, Barton *et al.* 1998; Pelegrí *et al.* 2005, 2006). Other studies have stressed the importance of the CVFZ as a barrier between waters of northern and southern origin and a region of water convergence and export (Barton 1987, Zenk *et al.* 1991, Gabric *et al.* 1993). However, here we have shown that the continental slope current system, between the sea surface and at least 500 m, may indeed break most of these major constraints. The slope system plays a significant role both in cross-CVFZ transfer and in the ventilation of the GD region, therefore being a significant pathway of water-mass exchange between tropical and subtropical gyres.

#### ACKNOWLEDGEMENTS

This research has been funded by the Spanish Ministerio de Ciencia e Innovación through projects MOC2 (CTM2008-06438-C02-01), ARGO-CANARIAS (CTM2009-08462-E) and TIC-MOC (CTM2011-28867). JP-I has been supported through an FPI doctoral grant linked to MOC2. We are grateful to the technicians and crew of the R/V *Sarmiento de Gamboa* for their field support and to our cruise colleagues for many fruitful discussions. Special thanks are due to José Antonio Pozo, the chief technician during the CANOA08 cruise.

#### REFERENCES

- Arhan M., Mercier H., Bourles B., Gouriou Y., 1998. Hydrographic sections across the Atlantic at 7°30N and 4°30S. *Deep-Sea Res. Part I* 45: 829-872.
- Barton E.D. 1987. Meanders, eddies and intrusions in the Central Water Mass Front off NW Africa. *Oceanol. Acta* 10: 267-283.
- Barton E.D. 1989. The poleward undercurrent on the eastern boundary of the Subtropical North Atlantic. In: Neshyba S., Smith R.L., Mooers C.N.K. (eds.), *Poleward flows along Eastern Ocean Boundaries*. Springer-Verlag Lecture Note Series, pp. 82-95.
- Barton E.D. 1998. Eastern boundary of the North Atlantic: Northwest Africa and Iberia. In: Robinson A.R., Brink K.H. (eds.), *The Sea*. John Wiley and Sons Inc., New York, pp. 633-657.
- Csanady G.T. 1977. Intermittent full upwelling in Lake Ontario. *J. Geophys. Res.* 82: 397-419.
- Elmoussaoui A., Arhan M., Treguier A.M. 2005. Model-inferred upper ocean circulation in the eastern tropics of the North Atlantic. *Deep-Sea Res. Part A* 52: 1093-1120.
- Fraga F. 1974. Distribution des masses d'eau dans l'upwelling de Mauritanie. *Tethys* 6: 5-10.
- Gabric A.J., García L., VanCamp L., Nykjaer L., Eifler W., Schrimpf W. 1993. Offshore export of shelf production in the Cape Blanc (Mauritania) Gicant filament as derived from Coastal Zone Color Scanner imagery. *J. Geophys. Res.* 98: 4697-4712.
- Hagen E. 2001. Northwest African upwelling scenario. *Oceanol. Acta* 24: S113-S128.
- Hughes P., Barton E.D. 1974. Physical Investigations in the upwelling region of North West Africa on RRS Discovery cruise 48. *Tethys* 6: 43-52.
- Kartensen J., Stramma L., Visbeck M. 2005. Oxygen minimum zones in the eastern tropical Atlantic and Pacific Ocean. *Prog. Oceanogr.* 77: 331-350.
- Kawase M., Sarmiento J.L. 1985. Nutrients in the Atlantic thermocline. *J. Geophys. Res.* 90: 8961-8979.
- Klein B., Tomczak M. 1994. Identification of diapycnal mixing through optimum multiparameter analysis 2. Evidence of unidirectional diapycnal mixing in the front between North and South Atlantic Central Water. *J. Geophys. Res.* 99: 25,275-25,280.
- Lankhorst M., Fratantoni D., Ollitrault M., Richardson P., Send U., Zenk W. 2009. The mid-depth circulation of the northwestern tropical Atlantic observed by floats. *Deep-Sea Res. Part I* 56: 1615-1632.
- Lazaro C., Fernandes M.J., Santos A.M.P., Oliveira P. 2005. Seasonal and interannual variability of surface circulation in the Cape Verde region from 8 years of merged T/P and ERS-2 altimeter data. *Remote Sens. Environ.* 98: 45-62.
- Luyten, J. R., Pedlosky J., Stommel H. (1983), The ventilated thermocline, *J. Phys. Oceanogr.* 13: 292-309.
- Machín F., Hernández-Guerra A., Pelegrí J.L. 2006. Mass fluxes in the Canary Basin. *Prog. Oceanogr.* 70: 416-447.
- Machín F., Pelegrí J.L. 2009. Northward penetration of Antarctic intermediate water off Northwest Africa. *J. Phys. Oceanogr.* 39: 512-535.
- Machín F., Pelegrí J.L., Fraile-Nuez E., Vélez-Belchí P., López-Laatz F., Hernández-Guerra A. 2010. Seasonal Flow Reversals of Intermediate Waters in the Canary Current System East of the Canary Islands. *J. Phys. Oceanogr.* 40: 1902-1909.
- Mackas D.L., Denman K.L., Bennett A.F. 1987. Least-square multiple tracer analysis of water mass composition. *J. Geophys. Res.* 92: 2907-2918.
- Mason E., Colas F., Molemaker J., Shchepetkin A.F., Troupin C., McWilliams J.C., Sangrà P. 2011. Seasonal variability of the Canary Current: a numerical study. *J. Geophys. Res.* 116: C06001.
- Mittelstaedt E. 1976. On the currents along the Northwest African coast south of 22° North. *Dt. Hydrogr. Z.* 29: 97-117.
- Mittelstaedt E. 1983. The upwelling area off Northwest Africa. A description of phenomena related to coast upwelling. *Prog. Oceanogr.* 12: 307-331.
- Mittelstaedt M. 1991. The ocean boundary along the northwest African coast: Circulation and oceanographic properties at the sea surface. *Prog. Oceanogr.* 26: 307-355.
- Nykjaer L., Van Camp L. 1994. Seasonal and interannual variability of coastal upwelling along northwest Africa and Portugal from 1981 to 1991. *J. Geophys. Res.* 99: 14797-14207.
- Pastor M.V., Pelegrí J.L., Hernández-Guerra A., Font J., Salat J., Emelianov M. 2008. Water and nutrient fluxes off Northwest Africa. *Cont. Shelf Res.* 28: 915-936.
- Pastor M.V., Peña-Izquierdo J., Pelegrí J.L., Marrero-Díaz A. 2012. A Meridional changes in water properties off NW Africa during November 2007/2008. *Cienc. Mar.* 38(1B): 223-244.
- Pelegrí J.L., Arístegui J., Cana L., González-Dávila M., Hernández-Guerra A., Hernández-León S., Marrero-Díaz A., Santana-Casiano M. 2005. Coupling between the open ocean and the coastal upwelling region off northwest Africa: Water recirculation and offshore pumping of organic matter. *J. Mar. Syst.* 54: 3-37.
- Pelegrí J.L., Marrero-Díaz A., Ratsimandresy A.W. 2006. Nutrient irrigation of the North Atlantic. *Prog. Oceanogr.* 70: 366-406.
- Peterson R.G., Stramma L. 1991. Upper-level circulation in the South Atlantic Ocean. *Prog. Oceanogr.* 26: 1-73.
- Richardson P.L., Walsh D. 1986. Mapping climatological seasonal variations of surface currents in the tropical Atlantic using ship drifts. *J. Geophys. Res.* 91: 10537-10550.
- Rodríguez-Marroyo R., Viúdez A., Ruiz S. 2011. Vortex merger in oceanic tripoles. *J. Phys. Oceanogr.* 41: 1239-1251.
- Siedler G., Zangenberg N., Onken R., Morlière A. 1992. Seasonal Changes in the Tropical Atlantic Circulation: Observation and Simulation of the Guinea Dome. *J. Geophys. Res.* 97: 703-715.
- Stark J. D., Donlon C. J., Martin M. J., McCulloch M. E., 2007. OSTIA: An operational, high resolution, real time, global sea surface temperature analysis system. Proc. Oceans '07, Marine Challenges: Coastline to Deep Sea, Aberdeen, Scotland, IEEE/OES, 1-4.

- Stramma L., Schott F. 1999. The mean flow field of the tropical Atlantic Ocean. *Deep-Sea Res. II* 46: 279-303.
- Stramma L., Hüttl D., Schafstall J. 2005. Water masses and currents in the upper tropical northeast Atlantic off northwest Africa. *J. Geophys. Res.* 110: 12006.
- Stramma L., Brandt P., Schafstall J., Schott F., Fischer J., Körtzinger A. 2008. Oxygen minimum zone in the North Atlantic south and east of the Cape Verde Islands. *J. Geophys. Res.* 113: C04014.
- Tomczak M. 1972. Problems of physical oceanography in coastal upwelling investigations. *Geoforum* 11: 23-34.
- Tomczak M., Hughes P. 1980. Three-dimensional variability of water masses and currents in the Canary Current upwelling region. "Meteor" *Forschungs-Ergebnisse A* 21: 1-24.
- Tomczak M. 1981. A multiparameter extension of temperature/salinity diagram techniques for the analysis of non-isopycnal mixing. *Prog Oceanogr.* 10: 147-171.
- Tomczak M., Large D.G.B. 1989. Optimum multiparameter analysis of mixing in the thermocline of the eastern Indian Ocean. *J. Geophys. Res.* 94: 16141-16149.
- Van Camp L., Nykjaer L., Mittelstaedt E., Schlittenhardt P. 1991. Upwelling and boundary circulation off Northwest Africa as depicted by infrared and visible satellite observations. *Prog. Oceanogr.* 26: 357-402.
- Voituriez B., Chuchla R. 1978. Influence of the Southern Atlantic Central water on the distribution of salinity and oxygen in the northeast tropical Atlantic Ocean. *Deep-Sea Res.* 25: 107-117.
- Zenk W., Klein B., Schröder M. 1991. Cape Verde frontal zone. *Deep-Sea Res.* 38: S505-S530.

Received February 10, 2011. Accepted November 30, 2011.  
Published online August 3, 2012.